Chinese Journal of Chemical Engineering 28 (2020) 2778–2784

Contents lists available at ScienceDirect

Chinese Journal of Chemical Engineering

journal homepage: www.elsevier.com/locate/CJChE

Article

A high propylene productivity over B_2O_3/SiO_2@honeycomb cordierite catalyst for oxidative dehydrogenation of propane

Yuxi Zhou, Yang Wang, Wenduo Lu, Bing Yan, Anhui Lu *

State Key Laboratory of Fine Chemicals, Liaoning Key Laboratory for Catalytic Conversion Carbon Resources, School of Chemical Engineering, Dalian University of Technology, Dalian 116024, China

ARTICLE INFO

Article history:
Received 22 June 2020
Received in revised form 18 July 2020
Accepted 19 July 2020
Available online 27 August 2020

Keywords:
Oxidative dehydrogenation
Boron-based catalyst
Alkane
Propylene
Monolith
High GHSV

ABSTRACT

Boron-based metal-free catalysts for oxidative dehydrogenation of propane (ODHP) have drawn great attention in both academia and industry due to their impressive activity and olefin selectivity. Herein, the SiO_2 and B_2O_3 sequentially coated honeycomb cordierite catalyst is designed by a two-step wash-coat method with different B_2O_3 loadings (0.1%–10%) and calcination temperatures (600, 700, 800 °C). SiO_2 obtained by TEOS hydrolysis acts as a media layer to bridge the cordierite substrate and boron oxide *via* abundant Si—OH groups. The well-developed straight channels of honeycomb cordierite make it possible to carry out the reactor under high gas hourly space velocity (GHSV) and the thin wash-coated B_2O_3 layer can effectively facilitate the pore diffusion on the catalyst. The prepared B_2O_3/SiO_2@HC monolithic catalyst exhibits good catalytic performance at low boron oxide loading and achieves excellent propylene selectivity (86.0%), olefin selectivity (97.6%, propylene and ethylene) and negligible CO_2 (0.1%) at 16.9% propane conversion under high GHSV of 345,600 ml·(g B_2O_3)$^{-1}$·h^{-1}, leading to a high propylene space time yield of 15.7 g C_3H_6·(g B_2O_3)$^{-1}$·h^{-1} by suppressing the overoxidation. The obtained results strongly indicate that the boron-based monolithic catalyst can be properly fabricated to warrant the high activity and high throughput with its high gas/surface ratio and straight channels.

1. Introduction

Propylene is one of the most important chemical building blocks [1]. The production of propylene from dehydrogenation of propane offers an important route for the value-added utilization of shale gas and the diversification in olefin supply. It could release the dependence of petroleum resources and accelerate the economic benefit development [2]. The oxidative dehydrogenation of propane (ODHP) has attracted great attention due to the lower energy consumption, anti-carbon deposition and equilibrium limit broken in propane conversion [3–5]. In the past decades, a variety of metal-based catalysts such as vanadium, nickel, iron, chrome and cesium-based catalysts, have been wildly studied for ODHP, which however suffered from poor propylene selectivity (less than 60% at a propane conversion of ~20%) because of over-oxidation of olefins [6–10].

Boron-based metal free catalysts for ODHP are burgeoning in recent years due to the impressive propylene selectivity [11–15]. In the previous work, we reported that the edge hydroxylated boron nitride (BNOH) efficiently catalyzed ODHP, reaching a propylene selectivity of 80.2% with a little CO_2 (0.5%) at propane conversion of 20.6%. On the basis of understanding the reaction mechanism, B_2O_3/SBA-15 catalyst has been prepared, which performed higher catalytic activity because the abundant tricoordinated boroxol and hydroxylated linear boron species presented as active sites while the formation of B—O—Si bonds effectively anchored the boron species [16]. Later on, B_2O_3 supported on commercial SiO_2 (specific surface area of 300 $m^2 \cdot g^{-1}$) was also reported [17]. The high activity, olefin selectivity and commercial availability of B_2O_3 make the supported boron oxide catalyst being attractive candidate for industrial application.

Despite the promising advances of particulate boron-based catalysts in ODHP reaction, the problems such as high pressure drop of the catalyst packing and poor mass transfer in the catalyst pellets may limit their large scale application [18,19].To overcome these shortcomings, it is particularly desirable to develop catalysts that possess both excellent catalytic performance and enhanced mass transfer. Monolithic honeycomb ceramic catalyst with well-developed straight channels is capable to facilitate the active phase dispersion and efficient use of the catalyst, narrow the residence time differences and lower the pressure drop under high space velocity [20]. Owing to these advantages, monolithic honeycomb ceramic catalysts have been proven applicable to many fields such as the destruction of organic compounds [21], low temperature CO catalytic oxidation [22], selective catalytic reduction of NO_x [23] and catalytic combustion [24]. Among several options, cordierite honeycomb monolith ($2MgO–2Al_2O_3–5SiO_2$) is the most popularly used catalyst support, due to the excellent hydrothermal stability, high mechanical stability and plasticity [21,25–27].

* Corresponding author.
E-mail address: anhuilu@dlut.edu.cn (A. Lu).

https://doi.org/10.1016/j.cjche.2020.07.040
1004-9541/

Herein, we prepared monolithic cordierite honeycomb catalyst by a two-step wash-coating of SiO_2 and B_2O_3, which exhibited good catalytic activity and high propylene selectivity for ODHP. The advantages of monolithic structure were also discussed on the basis of catalytic performance under high GHSV.

2. Materials and Methods

2.1. Catalyst preparation

The honeycomb cordierite (denoted as HC, non-metal chemical machinery plant co. LTD, Yixing, Jiangsu) was cleaned by HNO_3 (4 mol·L^{-1}), then washed by deionized water until pH = 7, and followed by drying and 600 °C calcination for 2 h. The pretreated cordierite was dipped into the SiO_2 sol (TEOS ($C_8H_{20}O_4Si$)/H_2O/Ethanol = 0.6/5/2, pH ~2.5, hydrolyzation at 60 °C for 12 h [28]) for 10 min until the air inside the channels were removed, then aged in a sealed container at 30 °C for 12 h. The wash-coated SiO_2@HC was further dried at 50 °C for 12 h and calcined at 800 °C for 2 h before use.

As a typical example, the supported B_2O_3 on SiO_2@HC catalyst with the B_2O_3 loading of 5% was obtained by dipping the SiO_2@HC support into boric acid solution with H_3BO_3 concentration of 1 mol·L^{-1} at 65 °C for 10 min until the air bubbles disappeared, then dried at 50 °C for 12 h. Subsequently, the sample was calcined at 700 °C for 2 h to produce the supported B_2O_3/SiO_2@HC catalysts. The loading amount of B_2O_3 of the catalyst was calculated by the equation of wt% = $(m - m_0) / m$, where wt% stands for the B_2O_3 loading, m and m_0 are the mass of B_2O_3/SiO_2@HC and SiO_2@HC, respectively [23]. In addition, the pretreated cordierite was crushed into powder, then loaded with SiO_2 and B_2O_3 by impregnation, to prepare the powder samples, which are denoted as HC-p, SiO_2@HC-p and B_2O_3/SiO_2@HC-p, respectively. Supported BPO_4 catalyst on cordierite was prepared by dipping pretreated cordierite into the mixture of 0.3 mol·L^{-1} H_3BO_3 solution and H_3PO_4 (mole rate B/P = 1) for 10 min until air bubbles disappeared, then dried at 50 °C for 12 h. Subsequently, the sample was calcined at 700 °C for 2 h to produce 4% BPO_4@HC.

2.2. Characterization

The honeycomb monolith and catalysts were characterized by scanning electron microscopy (SEM) and X-ray powder diffraction (XRD). The SEM investigations were carried out with a Hitachi FESEM SU8220 instrument to examine the cross section of the monolithic B_2O_3/SiO_2@HC. The element chemical analysis was implemented with a NOVA Nano SEM 450 instrument. A layer of gold film was deposited on the catalyst to improve the electric conductivity. The XRD patterns were recorded on PANalytical X'Pert3 Powder diffractometer using Cu K_α radiation (λ = 0.15406 nm). The tube voltage was 40 kV, and the current was 40 mA.

2.3. Activity test

The catalytic tests were carried out with the entire monolith (600 cpsi, dimeter: 11 mm, length: 15 mm) placed inside a quartz reactor (Ø = 12 mm). The feed flow consisted of C_3H_8, O_2, N_2 (C_3H_8: O_2:N_2 = 1:1.5:3.5) with the total flow rate of 48 ml·min^{-1}, 96 ml·min^{-1} and 144 ml·min^{-1}, and the bed temperature was varied in the range of 450 °C–540 °C. The temperature was measured by a thermocouple placed at the inlet of the catalyst bed. The SiO_2@HC was used for blank test. Both reactants and products were analyzed by an online gas chromatograph (Techcomp, GC 7900). A GDX-102 and molecular sieve 5A

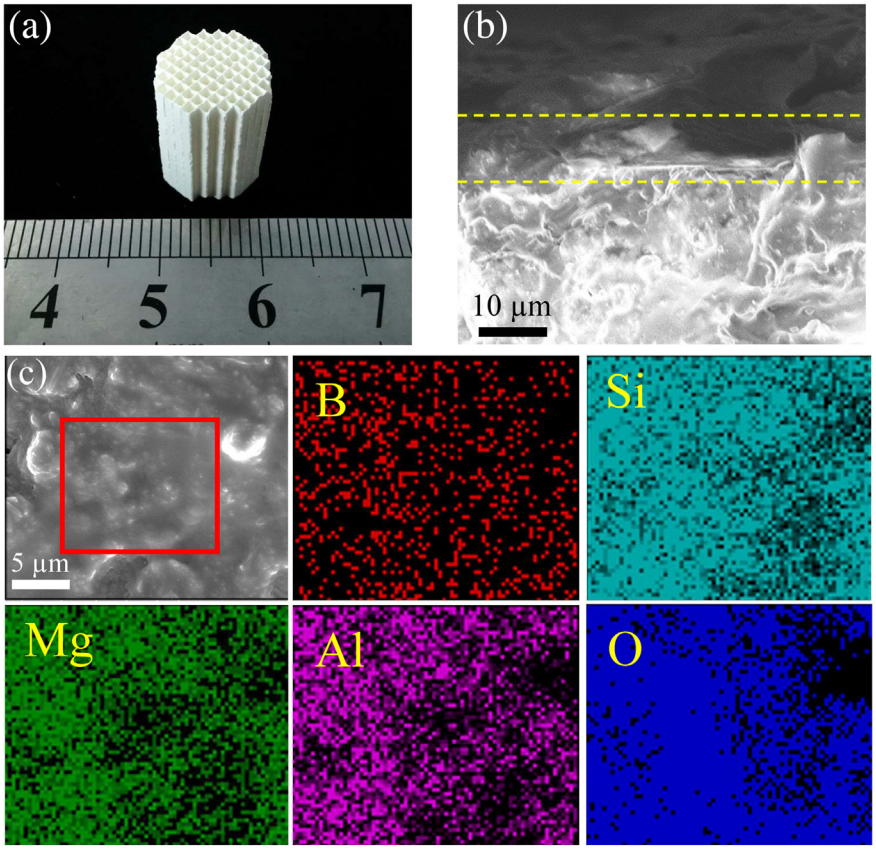

Fig. 1. (a) Optical photograph and (b) SEM images of the cross-section of monolithic B_2O_3/SiO_2@HC catalyst; (c) SEM image of the top view and the EDS mappings over the indicated zone.

column, connected to a TCD were used to analyze the O_2, N_2, C_3H_8, C_3H_6, C_2H_4, CO, and CO_2.

The Carberry number [29,30], which indicates the influence of external diffusion on the rate of reaction, was much smaller than 0.05. Therefore, the influence of external gas–solid mass transfer on the reaction rate was excluded.

The propane conversion was calculated as the number of carbon moles converted divided by the number of carbon moles in the feed gas. Selectivity was calculated as the number of carbon moles in the product divided by the number of carbon moles reacted. The propylene productivity was defined as the grams of propylene produced per gram boron oxide on the catalyst per hour. The carbon balance was kept in the range of 95%–100% for all reaction process. To account for the volume expansion in the reaction, nitrogen was used as the internal standard.

3. Results and Discussion

3.1. The structural features of the SiO_2 and B_2O_3 sequentially coated honeycomb cordierite catalyst

As shown in Fig. 1a, the supported B_2O_3 on SiO_2 pre-coated cordierite honeycomb ceramic catalyst (B_2O_3/SiO_2@HC) exhibited a honeycomb structure with parallel square channels (600 cells per square inch) and 0.24 mm wall thickness. The morphology of B_2O_3/SiO_2@HC catalyst was investigated by SEM at the cross-section (Fig. 1b), where the SiO_2-B_2O_3 layer was clearly observed on the cordierite substrate. Furthermore, the EDS mapping showed the investigated B_2O_3 uniformly distributed on the surface of the coating layer (Fig. 1c).

The XRD measurements were carried out using the powder samples. The XRD patterns for B_2O_3/SiO_2@HC-p, SiO_2@HC-p and HC-p are shown in Fig. 2. The three samples showed the signals mainly assigned to cordierite, while the sample B_2O_3/SiO_2@HC-p showed two peaks centered at 14.5° and 27.7° which were attributed to B_2O_3 (ICDD: 00-006-0297), confirming the formation of B_2O_3 phase. However, no peak belonged to SiO_2 was detected for the sample SiO_2@HC-p and the B_2O_3/SiO_2@HC-p, probably due to the small loading amount and amorphous nature of SiO_2.

The catalyst structure stability remains an important inspection parameter for the monolithic catalyst that the coating layer usually detaches from the support, leading to the deactivation of catalyst [31,32]. Therefore, the adhesion test was implemented by sonicating in petroleum ether for 150 min (30 min for each time followed by drying at 50 °C for 1 h). The mass losses of the five tests are almost zero.

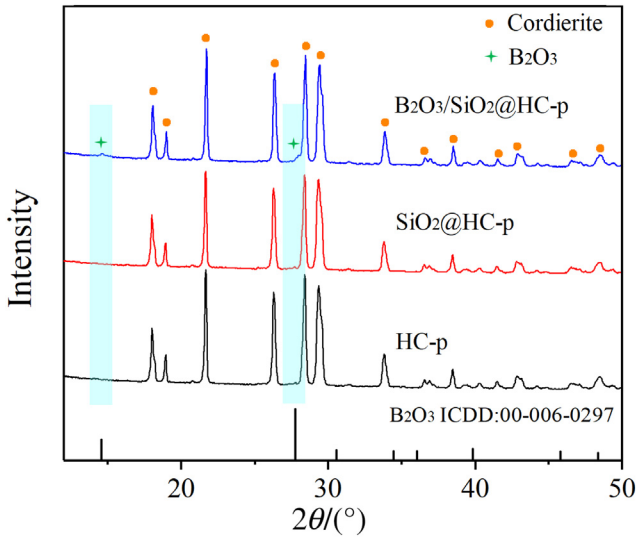

Fig. 2. XRD patterns for the powder samples of HC-p, SiO_2@HC-p and B_2O_3/SiO_2@HC-p.

These results showed the excellent adhesion of the coating layer on the cordierite, indicating the strong interaction between B_2O_3 and the SiO_2@HC support.

3.2. Optimization of the B_2O_3/SiO_2@HC catalyst

The effect of temperature on catalyst activity and products selectivity was investigated over B_2O_3/SiO_2@HC catalyst, as shown in Fig. 3a and b. The presence of B_2O_3 largely promoted the catalytic activity as compared to the SiO_2@HC support. The conversion of propane approached 16.0% at 500 °C, with high selectivity of olefin, *e.g.* C_3H_6 (84.9%), C_2H_4 (8.0%), and small amount of CO_2 (0.3%), achieving a propylene yield of 13.6%, whereas SiO_2@HC showed little activity. Furthermore, a series of B_2O_3/SiO_2@HC catalysts with varied loadings or calcination temperatures (denoted as X% B_2O_3/SiO_2@HC and B_2O_3/SiO_2@HC-*T*, respectively) were prepared in order to optimize the catalytic performance. As shown in Fig. 3c, raising the loading of B_2O_3 from 0.1%–1%, the catalytic activity increased, with propane conversion increasing from 2.8% to 17.7% at 500 °C, and the catalyst activity did not depend on B_2O_3 loading in the range from 1% to 5%, possibly due to the similar amount of accessible active sites. However, when the B_2O_3 loading increased to 10%, the activity of the catalyst decreased. Fig. 3d shows that catalysts calcined at 600 °C and 700 °C exhibited similar activity. However, when the catalyst was calcined at high temperature of 800 °C, its propane conversion was down to approximately 8% even at the reaction temperature of 500 °C. This conversion value was much lower than that over the catalysts calcined at 600 °C and 700 °C. As a result, the B_2O_3/SiO_2@HC catalyst with 5% B_2O_3 loading and calcined at 700 °C was used for the following investigation. These results confirm that B_2O_3 is the active phase for ODHP, which was consistent with our previous work [16]. Thermal treatments during calcination or under reaction condition may cause B_2O_3 vitrification or densification [33,34], causing the loss of accessible surface B—OH groups. Therefore, B_2O_3 coated firmly on the cordierite channel walls and calcined properly are important for the design of boron-based monolithic catalysts.

The catalytic stability test of B_2O_3/SiO_2@HC is shown in Fig. 4. The conversion of propane (~16%), the selectivity of propylene (84.5%) and ethylene (6.5%) were constant at 500 °C for 20 h on stream with no catalyst weight loss, demonstrating that after calcination at high temperature, active boron species were well anchored on SiO_2@HC. In comparison, the stability test was conducted over a control catalyst, *i.e.* 5% B_2O_3@HC, however, 10% B_2O_3 component weight loss was found after 20 h operation. The results mentioned above suggest that the bare cordierite was insufficient for boron immobilization. The reason could be that commercial cordierite honeycomb is usually produced after calcination at high temperature of ~1400 °C, causing its surface inertness with limited anchoring M—OH groups (M═Si, Mg, Al). To solve this problem, the cordierite support was modified by an additional silica coating layer which can attach firmly on the cordierite substrate possibly by forming Si—O—Al, Si—O—Mg, Si—O—Si bonds, and attach to the boron oxide layer *via* Si—O—B bonds. In this way, the silica layer, which has been confirmed inert toward ODHP, was used as the media layer to bridge the cordierite and boron oxide *via* the abundant Si—OH groups, and thus enhancing the catalyst thermal stability and meanwhile, tightly bridging the B_2O_3 layer and the substrate [16,35].

Recently, *h*-BN and BPO_4 have been realized as the active catalysts for ODH of propane [36]. To better clarify the advantages of B_2O_3 monolithic catalyst, *h*-BN/Cordierite [37] and the BPO_4@HC with the same boron loading were taken into comparison. The 3% *h*-BN/Cordierite catalyst was prepared by CVD with H_3BO_3 and urea as precursors calcinating at 1000 °C, and the 4% BPO_4@HC catalyst was prepared by dipping in the solution of H_3PO_4 and H_3BO_3 followed by calcination (details see Section 2.1). All of the three monolithic catalysts exhibited similar structure with straight channels of 600 cpsi and was test under a flow rate of 48 ml·min^{-1}. Fig. 5 shows the propane conversion curve as a function of temperature over the three samples, the activity

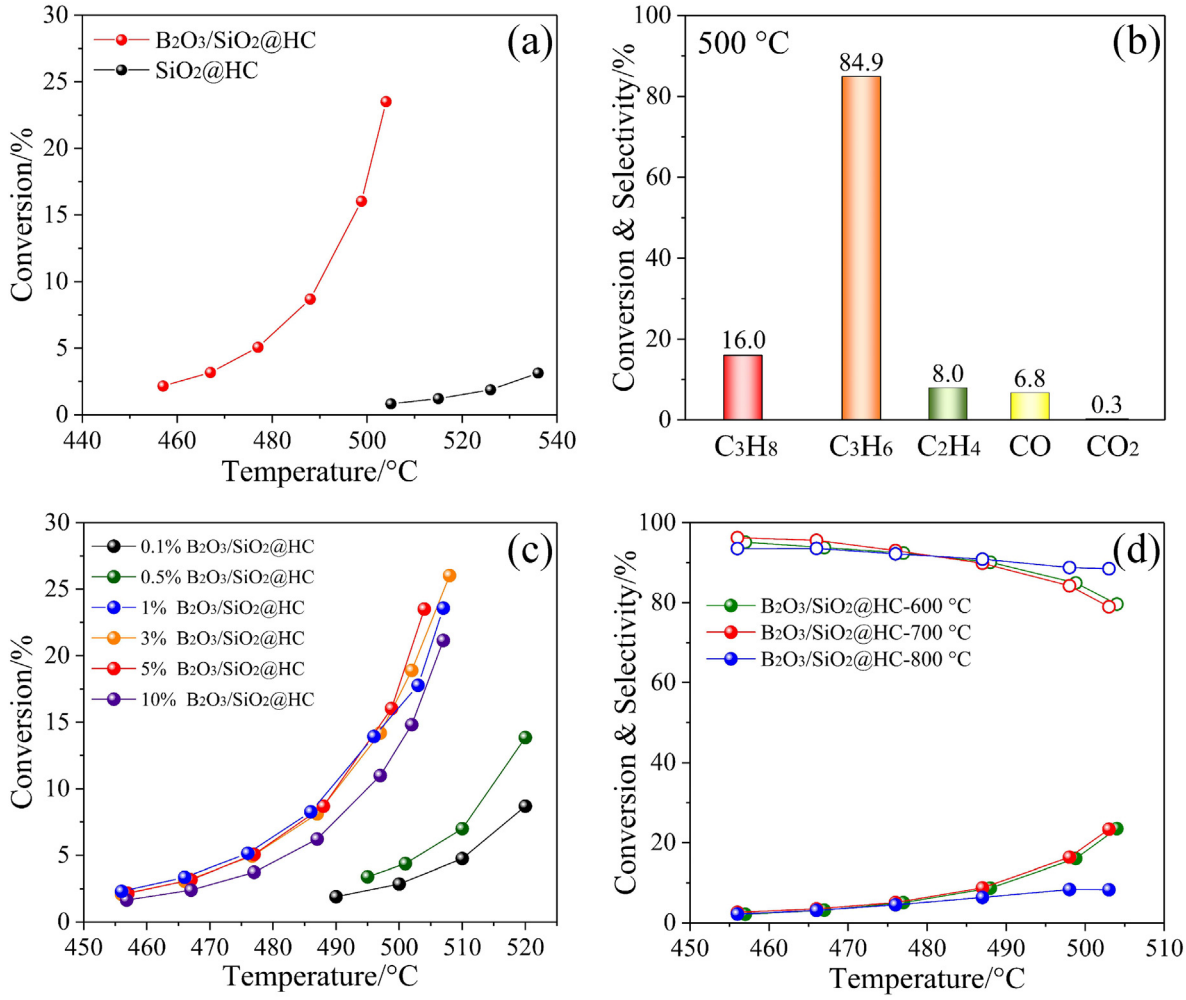

Fig. 3. a) The influence of temperature on propane conversion over the indicated samples; b) The propane conversion and product distribution at 500 °C over B_2O_3/SiO_2@HC catalyst; c) The propane conversion as a function of temperature over B_2O_3/SiO_2@HC catalyst with different loadings; d) The propane conversion (solid) and propylene selectivity (hollow) as a function of temperature over B_2O_3/SiO_2@HC-*T* catalysts. Reaction conditions: gas feed, 16.7 vol% C_3H_8, 25.0 vol% O_2, N_2 balance; flow rate 48 ml·min^{-1}.

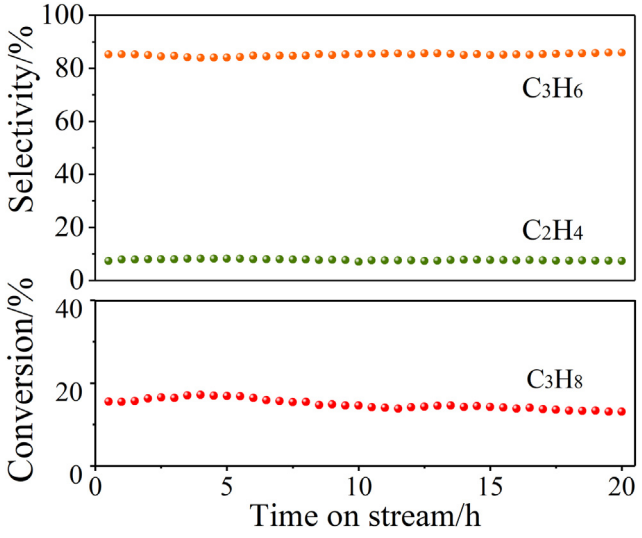

Fig. 4. The stability test over B_2O_3/SiO_2@HC catalyst at 500 °C. Reaction conditions: gas feed, 16.7 vol% C_3H_8, 25.0 vol% O_2, N_2 balance; flow rate 48 ml·min^{-1}.

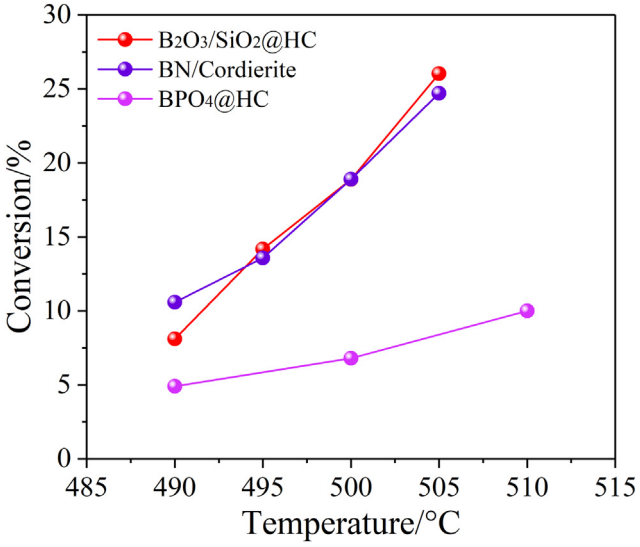

Fig. 5. The influence of temperature on propane conversion over the B_2O_3/SiO_2@HC, the *h*-BN/Cordierite and the BPO_4@HC catalysts. Reaction condition: gas feed, 16.7 vol% C_3H_8, 25.0 vol% O_2, N_2 balance; flow rate 48 ml·min^{-1}.

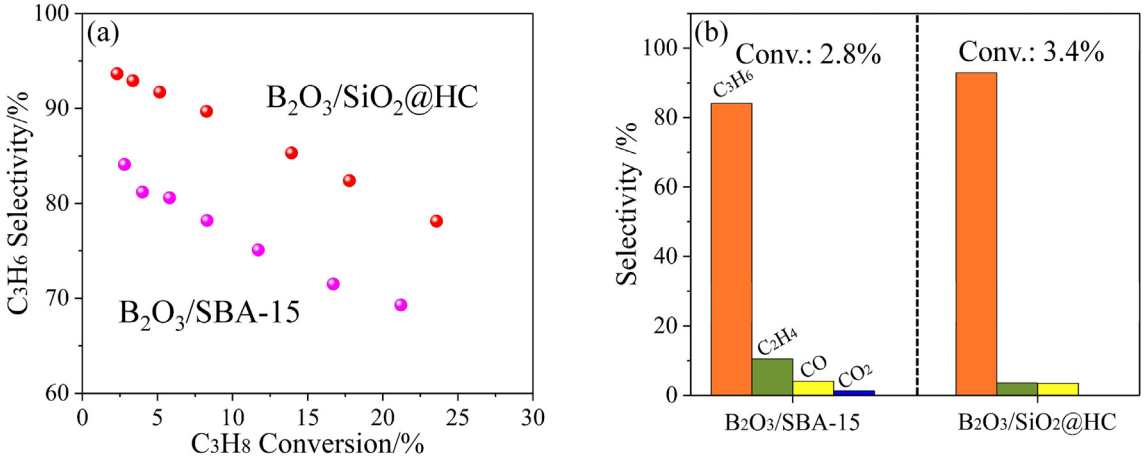

Fig. 6. The catalytic performance of the B_2O_3/SBA-15 and the B_2O_3/SiO_2@HC: propylene selectivity as a function of propane conversion (a), and products distribution at similar propane conversion (b). Reaction condition: gas feed, 16.7 vol% C_3H_8, 25.0 vol% O_2, N_2 balance; flow rate 48 ml·min^{-1}.

of *h*-BN/Cordierite was similar to that of B_2O_3/SiO_2@HC, indicating a similar amount of active sites present on these two catalysts. However, an induction period of 3 h is necessarily used for the *h*-BN/Cordierite to reach the optimal performance. Moreover, the BPO_4@HC shows the lowest activity compared to B_2O_3/SiO_2@HC and *h*-BN/Cordierite. It should be pointed out that the tricoordinated BO species has been proposed as the active sites of the boron-based catalyst over ODHP [16]. In the case of BPO_4, boron species are presents as tetracoordinated. Overall, the B_2O_3/SiO_2@HC could be recognized as a competitive catalyst in ODHP.

3.3. Effect of catalyst support on catalytic performance

To illustrate the role of catalyst structure of B_2O_3/SiO_2@HC, the B_2O_3/SBA-15 catalyst with the same B_2O_3 loading weight was taken as comparison. The propylene selectivity as a function of propane conversion was plotted in Fig. 6a and the products selectivity comparison at low propane conversion was shown in Fig. 6b. It shows that the selectivity of the C_3H_6 was 92.9% (Sel_{olefin} ~96.5%) and CO_2 was not detected over the B_2O_3/SiO_2@HC and the selectivity of the C_3H_6 and CO_2 over the B_2O_3/SBA-15 was 84.1% and 1.3% (Sel_{olefin} ~94.6%) [16], respectively. Furthermore, the propylene selectivity of B_2O_3/SiO_2@HC (92%) is higher than other SiO_2 supported boron oxide catalyst such as B/SiO_2 (77%) [17] at similar propane conversion. These results show that the monolithic B_2O_3/SiO_2@HC was much more selective toward propylene than the other SiO_2 supported pellet catalyst at similar propane conversions. These results suggested that the catalyst supports may have great impact on the product distribution of the resultant catalysts. Because the monolithic structure allows a uniform flow distribution facilitating the utilization of the active component, and the catalytic layer wash-coated on the monolithic wall shorten the diffusion paths so that the overoxidation was restrained. On the other hand, the negative effect of SiO_2 was reported on propylene selectivity for *h*-BN and B/SiO_2 catalysts [17,30]. However, the SiO_2 coating layer on the monolithic support showed no negative effect on selectivity but largely improved the catalyst stability.

To determine the key factor of high selectivity, the space velocity dependence was investigated over B_2O_3/SiO_2@HC at a similar propane conversion that adjusted by slightly varying the reaction temperature. As shown in Fig. 7a and Table 1, the product distribution depended on the space velocity. With a propane conversion of ~16.0%, olefin selectivity increased from 92.9% to 97.6% as the space velocity increased. At the highest GHSV used, the selectivity of CO_2

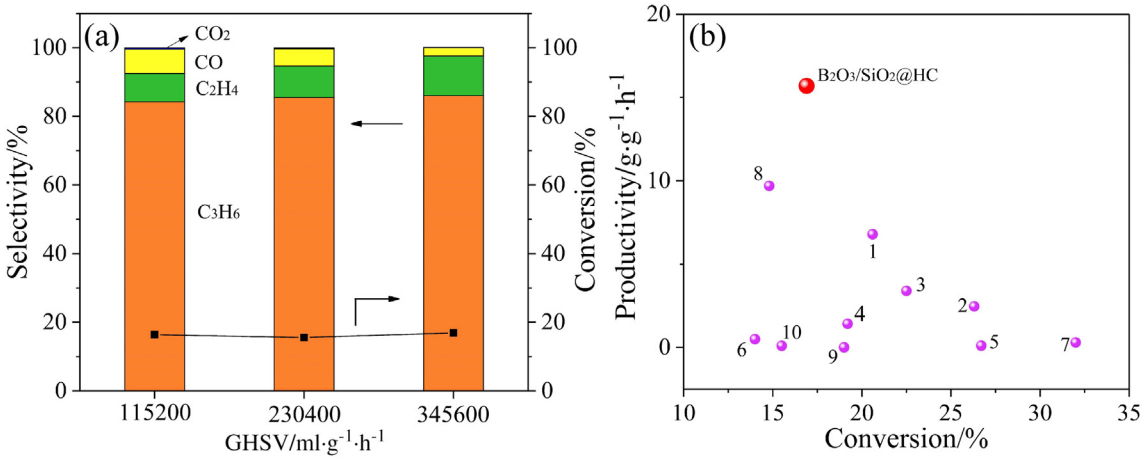

Fig. 7. (a) Effect of GHSV on the propane conversion and products selectivity over the B_2O_3/SiO_2@HC catalyst. (b) The comparison of propylene productivity between our work to the literatures. For better comparison, the productivity was normalized by the loading amount of active species. (1 [11], 2 [38], 3 [39], 4 [10], 5 [9], 6 [40], 7 [41], 8 [16], 9 [14], 10 [42].) Reaction conditions: gas feed, 16.7 vol% C_3H_8, 25.0 vol% O_2, N_2 balance.

Table 1
Catalytic performance of B_2O_3/SiO_2@HC catalyst under different GHSV

GHSV/ml·(g B_2O_3)$^{-1}$·h^{-1}	Temp./°C	Conv./%	Selectivity/%			
			C_3H_6	C_2H_4	CO	CO_2
115,200	500	16.0	84.9	8.0	6.8	0.3
230,400	520	15.6	85.5	9.2	5.1	0.2
345,600	535	16.9	86.0	11.6	2.3	0.1

was as low as 0.1%, reaching a space time yield of propylene as 15.7 g $C_3H_6\cdot(g\ B_2O_3)^{-1}\cdot h^{-1}$. This result is better than that over traditional metal oxide catalysts and also better than that over the most of boron-based catalysts (Fig. 7b).

4. Conclusions

In conclusion, the honeycomb cordierite monolithic B_2O_3/SiO_2@HC catalyst was designed and prepared by a two-step coating method. A high selectivity toward olefin (97.2%) and negligible production of CO_2 (0.1%) under high space velocity gave a high propylene productivity of 15.7 g $C_3H_6\cdot(g\ B_2O_3)^{-1}\cdot h^{-1}$ for ODHP. The promising performance of the catalyst was attributed to not only the efficient dispersion and firm attachment of the catalytically active B_2O_3 layer on the modified SiO_2@HC support, but also the improved mass transfer brought by the honeycomb structure. Overall, the SiO_2- and B_2O_3-coated honeycomb cordierite monolith could be potentially recognized for industrial application of ODHP.

Acknowledgements

This study was supported by State Key Program of National Natural Science Foundation of China (21733002), Joint Sino-German Research Project (21761132011), Cheung Kong Scholars Programme of China (T2015036).

References

[1] A. Corma, F.V. Melo, L. Sauvanaud, F. Ortega, Light cracked naphtha processing: controlling chemistry for maximum propylene production, *Catal. Today* 107-108 (2005) 699–706.
[2] J.J. Sattler, J. Ruiz-Martinez, E. Santillan-Jimenez, B.M. Weckhuysen, Catalytic dehydrogenation of light alkanes on metals and metal oxides, *Chem. Rev.* 114 (2014) 10613–10653.
[3] O. Schwarz, P.Q. Duong, G. Schäfer, R. Schomäcker, Development of a microstructured reactor for heterogeneously catalyzed gas phase reactions: part I. Reactor fabrication and catalytic coatings, *Chem. Eng. J.* 145 (2009) 420–428.
[4] C. Trionfetti, I.V. Babich, K. Seshan, L. Lefferts, Formation of high surface area Li/MgO-efficient catalyst for the oxidative dehydrogenation/cracking of propane, *Appl. Catal. A Gen.* 310 (2006) 105–113.
[5] J. Zhang, X. Liu, R. Blume, A.H. Zhang, R. Schlögl, D.S. Su, Surface-modified carbon nanotubes catalyze oxidative dehydrogenation of n-butane, *Science* 322 (2008) 73–77.
[6] E.V. Kondratenko, O.V. Buyevskaya, M. Baerns, Characterization of vanadium-oxide-based catalysts for the oxidative dehydrogenation of propane to propene, *Top. Catal.* 15 (2001) 175–180.
[7] G. Xiong, J.N. Sang, Oxidative dehydrogenation of propane over nanodiamond modified by molybdenum oxide, *J. Mol. Catal. A Chem.* 392 (2014) 315–320.
[8] M. Khachani, M. Kacimia, A. Ensuque, J. Piquemal, C. Connan, F.B.M. Ziyad, Iron-calcium-hydroxyapatite catalysts: iron speciation and comparative performances in butan-2-ol conversion and propane oxidative dehydrogenation, *Appl. Catal. A Gen.* 388 (2010) 113–123.
[9] M.A.D. León, C.D.L. Santos, L. Latrónica, A.M. Cesio, C. Volzone, J. Castiglioni, M. Sergio, High catalytic activity at low temperature in oxidative dehydrogenation of propane with Cr-Al pillared clay, *Chem. Eng. J.* 241 (2014) 336–343.
[10] J.Z. Zhang, M. Sun, C.J. Cao, Q.H. Zhang, Y. Wang, H.L. Wan, Effects of acidity and microstructure on the catalytic behavior of cesium salts of 12-tungstophosphoric acid for oxidative dehydrogenation of propane, *Appl. Catal. A Gen.* 380 (2010) 87–94.
[11] L. Shi, D.Q. Wang, W. Song, D. Shao, W.P. Zhang, A.H. Lu, Edge hydroxylated boron nitride for oxidative dehydrogenation of propane to propylene, *ChemCatChem* 10 (2017) 1788–1793.
[12] J.M. Venegas, W.P. McDermott, I. Hermans, Serendipity in catalysis research: boron-based materials for alkane oxidative dehydrogenation, *Acc. Chem. Res.* 51 (2018) 2556–2564.
[13] P. Chaturbedy, M. Ahamed, M. Eswaramoorthy, Oxidative dehydrogenation of propane over a high surface area boron nitride catalyst: exceptional selectivity for olefins at high conversion, *ACS Omega* 3 (2018) 369–374.
[14] B. Yan, W.C. Li, A.H. Lu, Metal-free silicon boride catalyst for oxidative dehydrogenation of light alkanes to olefins with high selectivity and stability, *J. Catal.* 369 (2019) 296–301.
[15] J.A. Loiland, Zh. Zhao, A. Patel, P. Hazin, Boron-containing catalysts for the oxidative dehydrogenation of ethane/propane mixtures, *Ind. Eng. Chem. Res.* 58 (2019) 2170–2180.
[16] W.D. Lu, D.Q. Wang, Z.C. Zhao, W. Song, W.C. Li, A.H. Lu, Supported boron oxide catalysts for selective and low temperature oxidative dehydrogenation of propane, *ACS Catal.* 9 (2019) 8263–8270.
[17] A.M. Love, M.C. Cendejas, B. Thomas, W.P. McDermott, P. Uchupalanun, C. Kruszynski, S.P. Burt, T. Agbi, A.J. Rossini, I. Hermans, Synthesis and characterization of silica-supported boron oxide catalysts for the oxidative dehydrogenation of propane, *J. Phys. Chem. C* 123 (2019) 27000–27011.
[18] Z.Q. Zhang, J. Ding, R.J. Chai, G.F. Zhao, Y. Liu, Y. Lu, Oxidative dehydrogenation of ethane to ethylene: a promising CeO_2-ZrO_2-modified NiO-Al_2O_3/Ni-foam catalyst, *Appl. Catal. A Gen.* 550 (2018) 151–159.
[19] H. Yuan, Z.H. Sun, H.Y. Liu, B.S. Zhang, C.L. Chen, H.H. Wang, Z.M. Yang, J.S. Zhang, F. Wei, D.S. Su, Immobilizing carbon nanotubes on SiC foam as a monolith catalyst for oxidative dehydrogenation reactions, *ChemCatChem.* 5 (2013) 1713–1717.
[20] X.C. Gao, Y.J. Zhao, S.P. Wang, Y.L. Yin, B.W. Wang, X.B. Ma, A Pd-Fe/a-Al_2O_3/cordierite monolithic catalyst for CO coupling to oxalate, *Chem. Eng. Sci.* 66 (2011) 3513–3522.
[21] R.M. Heck, Su. Gulati, R.J. Farrauto, The application of monoliths for gas phase catalytic reactions, *Chem. Eng. J.* 82 (2001) 149–156.
[22] B. Kucharczyk, W. Tylus, J. Okal, J. Checmanowski, B. Szczygieł, The Pt-NiO catalysts over the metallic monolithic support for oxidation of carbon monoxide and hexane, *Chem. Eng. J.* 309 (2017) 288–297.
[23] T.Q. Zhou, L.D. Li, J. Cheng, Z.P. Hao, Preparation of binary washcoat deposited on cordierite substrate for catalytic applications, *Ceram. Int.* 36 (2010) 529–534.
[24] M. Zang, C.C. Zhao, Y.Q. Wang, X. Liu, Y. Cheng, S.Q. Chen, Low temperature catalytic combustion of toluene over three-dimensionally ordered $La_{0.8}Ce_{0.2}MnO_3$/Cordierite catalysts, *Appl. Sur. Sci.* 483 (2019) 355–362.
[25] B.M. Sollier, L.E. Gómez, A.V. Boix, E.E. Miró, Oxidative coupling of methane on cordierite monoliths coated with Sr/La_2O_3 catalysts. Influence of honeycomb structure and catalyst-cordierite chemical interactions on the catalytic behavior, *Appl. Catal. A: Gen.* 550 (2018) 113–121.
[26] J.K. He, S.Y. Chen, W.X. Tang, Y.L. Dang, P. Kerns, R. Miao, B. Dutta, P.X. Gao, S.L. Suib, Microwave-assisted integration of transition metal oxide nanocoatings on manganese oxide nanoarray monoliths for low temperature CO oxidation, *Appl. Catal. B Environ.* 255 (2019) 117766–117776.
[27] F.A.C. Oliveira, J.C. Fernandes, Mechanical and thermal behaviour of cordierite–zirconia composites, *Ceram. Int.* 28 (2002) 79–91.
[28] C. Agustín-Sáenz, M. Machado, A. Tercjak, Antireflective mesoporous silica coatings by optimization of water content in acid-catalyzed sol-gel method for application in glass covers of concentrated photovoltaic modules, *J. Colloid Interf. Sci.* 534 (2019) 370–380.
[29] H.R. Yue, Y.J. Zhao, L. Zhao, J. Lv, S.P. Wang, J.L. Gong, X.B. Ma, Hydrogenation of dimethyl oxalate to ethylene glycol on Cu/SiO_2/Cordierite monolithic catalyst: Enhanced internal mass transfer and stability, *AIChE J.* 58 (2012) 2798–2809.
[30] J.M. Venegas, I. Hermans, The influence of reactor parameters on the boron nitride-catalyzed oxidative dehydrogenation of propane, *Org. Process. Res. Dev.* 22 (2018) 1644–1652.
[31] Y.K. Kee, J.E. Hyun, C.K. Soon, H.J. Un, L.Y. Wang, Ru-coated metal monolith catalyst prepared by novel coating method for hydrogen production via natural gas steam reforming, *Catal. Today* 293 (2017) 129–135.
[32] M.R. Morales, M.P. Yeste, H. Vidal, J.M. Gatica, L.E. Cadus, Insights on the combustion mechanism of ethanol and *n*-hexane in honeycomb monolithic type catalysts: Influence of the amount and nature of Mn-Cu mixed oxide, *Fuel* 208 (2017) 637–646.
[33] J. Rockett, W.R. Foster, Phase relation in the system boron oxide silica, *J. Am. Ceram. Soc.* 48 (1965) 75–80.
[34] G. Ferlat, T. Charpentier, A.P. Seitsonen, A. Takada, M. Lazzeri, L. Cormier, G. Calas, F. Mauri, Boroxol rings in liquid and vitreous B_2O_3 from first principles, *Phys. Rev. Lett.* 101 (2008), 065504.
[35] L.D. Li, B. Xue, J.X. Chen, N.J. Gua, F.X. Zhang, D.X. Liu, H.Q. Feng, Direct synthesis of zeolite coatings on cordierite supports by *in situ* hydrothermal method, *Appl. Catal. A Gen.* 292 (2005) 312–321.
[36] W.D. Lu, X.Q. Gao, Q.G. Wang, W.C. Li, Z.C. Zhao, D.Q. Wang, A.H. Lu, Ordered macroporous boron phosphate crystals as metal-free catalysts for the oxidative dehydrogenation of propane, *Chinese J. Catal.* 41 (2020) 1837–1845.

[37] Y. Wang, W.C. Li, Y.X. Zhou, R. Lu, A.H. Lu, Boron nitride wash-coated cordierite monolithic catalyst showing high selectivity and productivity for oxidative dehydrogenation of propane, *Catal. Today* 339 (2020) 62–66.

[38] Y.M. Liu, W.L. Feng, L.C. Wang, Y. Cao, W.L. Dai, H.Y. He, K.N. Fan, Chromium supported on mesocellular silica foam (MCF) for oxidative dehydrogenation of propane, *Catal. Lett.* 106 (2006) 145–152.

[39] A. Ramireza, J.L. Hueso, R. Mallada, J. Santamaria, Microwave-activated structured reactors to maximize propylene selectivity in the oxidative dehydrogenation of propane, *Chem. Eng. J.* 393 (2020) 124746–124753.

[40] J.T. Grant, C.A. Carrero, F. Goeltl, J. Venegas, P. Mueller, S.P. Burt, S.E. Specht, W.P. McDermott, A. Chieregato, I. Hermans, Selective oxidative dehydrogenation of propane to propene using boron nitride catalysts, *Science* 354 (2016) 1570–1573.

[41] X.Q. Fan, D.D. Liu, Z. Zhao, J.M. Li, J. Liu, Influence of Ni/Mo ratio on the structure-performance of ordered mesoporous Ni-Mo-O catalysts for oxidative dehydrogenation of propane, *Catal. Today* 339 (2020) 67–78.

[42] P. Michorczyk, P. Kustrowski, P. Niebrzydowska, A. Wach, N.A. Wach, Catalytic performance of sucrose-derived CMK-3 in oxidative dehydrogenation of propane to propene, *Appl. Catal. A Gen.* 445-446 (2012) 321–328.